Proceedings of the PHOTON-2017 Conference, Geneva, Switzerland, 22 – 26 May 2017, edited by David d'Enterria, Albert de Roeck and Michelangelo Mangano, CERN Proceedings, Vol. 1/2018, CERN-Proceedings-2018-001 (CERN, Geneva, 2018)

Photoproduction of vector mesons in ultra-peripheral Pb-Pb interactions with ALICE

Christopher D. Anson, for the ALICE Collaboration
Creighton University, Omaha, NE, USA

Abstract
Cross section measurements for vector meson production in ultra-peripheral collisions (UPCs) provide important insight into nuclear gluon distributions, the production mechanisms of vector mesons and a better understanding of the early stages of heavy ion collisions. With data collected during LHC Run 1, ALICE measured vector meson production in ultra-peripheral Pb-Pb collisions at $\sqrt{s_{NN}} = 2.76$ TeV. Detector upgrades and improved triggers before LHC Run 2 will be discussed. These improvements have allowed a much higher statistics data set to be collected for UPCs at $\sqrt{s_{NN}} = 5.02$ TeV. The new data allow for more differential studies to be performed and to probe nuclear gluon distributions at lower values of Bjorken x. The most recent ALICE measurements of vector meson production for ρ^0, J/ψ, and ψ(2S) mesons will be presented along with comparisons to the latest available models.

Keywords
ALICE; UPC; vector mesons.

1 Introduction

Ultra-peripheral collisions (UPC) occur when two colliding particles pass by one another with an impact parameter, b, larger than the sum of the radii of the two particles: $b > R_1 + R_2$. Hadronic interactions are greatly suppressed in these collisions whereas long-range electromagnetic interactions between the nuclei may still proceed. These electromagnetic interactions are enhanced in Pb-Pb collisions compared to p-p collisions at the same energy because of the much larger charge of the Pb ions. The reason is that at ultra-relativistic energies, the electromagnetic field of each ion can be replaced by an equivalent flux of quasi-real photons. When a UPC event occurs, a photon from either nuclei may interact with either a photon from the other nucleus, the other nucleus as a whole or a single nucleon in the other nucleus, producing new particles. These interactions are referred to, respectively, as photon-photon interactions, photo-nuclear (coherent) interactions or photon-nucleon (incoherent) interactions. Vector mesons, such as ρ^0, J/ψ and ψ(2S) are commonly created in these processes. The equivalent flux of photons that may participate in UPC events is enhanced by a factor of 6724 for Pb-Pb collisions compared to p-p collisions due to the larger electric charge of the heavy ions. The energy spectrum of these photons reaches a maximum value which is proportional to the Lorentz factor of the colliding particles. Measurements of heavy ion interactions at the energies available at the LHC provide an ideal environment to study interactions in UPC events.

Measurements of ultra-peripheral collisions provide insight into both the production mechanisms for heavy vector mesons and the initial distribution of gluons inside nuclei. Cross sections for coherent photo-production of vector mesons are proportional to the square of the nuclear gluon distribution. Measurements at different rapidities and energies, both with and without accompanying photo-nuclear dissociation of the nuclei, provide experimental constraints for these distributions over a range of values of Bjorken x. The studies that can be performed at ALICE with Run 2 data will provide results at lower values of Bjorken x, where theoretical uncertainties in the nuclear gluon distribution are largest and experimental guidance is especially needed. Because different models may include different amounts of

https://doi.org/10.23727/CERN-Proceedings-2018-001.131

gluon shadowing and may incorporate different assumptions, measurements of differential cross sections, $d\sigma/dy$, can help distinguish between models.

The results presented in this paper focus on the most recent ALICE measurements of UPC events in Pb-Pb collisions. An overview of the detector configuration and triggers after the upgrade for Run 2 is provided in Sec. 2. In Sec. 3 new results and comparison to models are discussed for coherent vector meson production of ρ^0, and ψ(2S) at mid-rapidity and J/ψ at both forward and mid-rapidity.

2 ALICE detector and UPC triggers

The ALICE detector is optimized for measurements of heavy ion collisions produced at the LHC. Detailed overviews of the detector and its performance can be found in Refs. [1] and [2], respectively. The detectors currently used for UPC measurements include the Time Projection Chamber (TPC), Time-of-Flight (TOF) and Silicon Pixel Detector (SPD) at mid rapidities and the Muon Arm at backward rapidity. Additionally, the V0, ALICE Diffractive (AD) and Zero Degree Calorimeters (ZDC), which have components in both the forward and backward rapidity regions, are utilized. Each of these detectors are used either for tracking and particle identification, as part of the trigger for selecting UPC events, or in some cases both. The addition of the AD detector for Run 2 enhances the ability to suppress events that may contain hadronic interactions. A summary of the subdetectors, their rapidity coverage, function in UPC measurements and specific requirements are given in Table 1.

Table 1: Summary of ALICE UPC triggers for Run 2

Detector	**Rapidity**	**Function**	**Requirements**
	Central trigger		
TPC	$\|\eta\| < 0.9$	Tracking/PID	
TOF	$\|\eta\| < 0.9$	Trigger	≥ 2 back-to-back hits
SPD	$\|\eta\| < 1.4$ (outer), $\|\eta\| < 2.0$ (inner)	Trigger	≥ 2 back-to-back hits
V0[a]	$-3.7 < \eta < -1.7$, $2.8 < \eta < 5.1$	Trigger	V0A and V0C empty
AD[a]	$-7.0 < \eta < -4.9$, $4.8 < \eta < 6.3$	Trigger	ADA and ADC empty
	Forward trigger		
Muon Arm[b]	$-4.0 < \eta < -2.5$	Tracking/PID/Trigger	2 muons, $p_T > 1GeV$
V0[a]	$-3.7 < \eta < -1.7$, $2.8 < \eta < 5.1$	Trigger	Only V0A empty
AD[a]	$-7.0 < \eta < -4.9$, $4.8 < \eta < 6.3$	Trigger	ADA and ADC empty
SPD	$\|\eta\| < 1.4$ (outer), $\|\eta\| < 2.0$ (inner)	Trigger	No SPD hits

[a] V0 and AD have components on both the "A" side (V0A, ADA) and "C" side (V0C, ADC).

[b] The Muon Arm is located on the "C" side of ALICE in the backward rapidity region.

For UPC measurements at mid-rapidity, the TPC provides tracking and particle identification. The central UPC trigger requires back-to-back hits in the SPD near the beam pipe and back-to-back hits in the TOF, just outside of the TPC. This signal selects events with at least two back-to-back tracks. In central UPC events there should be no activity in the forward or backward regions of the detector. The V0 and AD detectors are therefore required to have no signal, effectively suppressing events with hadronic interactions. The ρ^0 analysis used a separate trigger class without the TOF requirement.

For UPC measurements at backward rapidity, the Muon Arm provides tracking and particle identification. In addition, it is used as part of the trigger by requiring only two muons with $p_T > 1.0$ GeV/c be identified. In this case the SPD is required to have no signal, indicating the central region of the detector is empty. The V0 opposite the Muon Arm and the AD on both sides are required to have no signal, providing a veto to suppress events with hadronic interactions. The other V0 lies in front of the Muon Arm so the muons may pass through it; it is excluded from the veto in the case of the forward UPC trigger. The ZDCs lie at very forward and backward rapidities and may be used to study UPC events

in which one or more of the colliding nuclei may photo-dissociate and emit neutrons. They will allow measurements at lower values of Bjorken x, providing tighter constraints on gluon distribution functions.

3 Latest results

Using Run 1 data, ALICE published measurements of ρ^0 [3] and ψ(2S) [4] at mid-rapidity and of J/ψ at both forward [5] and mid-rapidity [6] for Pb-Pb collisions at $\sqrt{s_{NN}} = 2.76$ TeV. The latest results, using Run 2 data, benefit from significantly higher statistics that were obtained because of higher luminosity, the addition of the AD detector to enhance the UPC triggers, and the higher energy of the collisions. The higher statistics allow for more differential measurements and smaller uncertainties, thereby providing improved constraints for models.

3.1 Coherent ρ^0

The coherent ρ^0 measurement is made in the $\pi^+\pi^-$ channel. The two pion invariant mass spectrum is shown in Fig. 1 (left). To extract the ρ^0 yield, a Söding fit of the form

$$\frac{d\sigma}{dm_{\pi\pi}} = |A \cdot BW + B + C \cdot e^{i\phi} \cdot BW|^2 + N \cdot Pol6 \tag{1}$$

was performed both with and without the ρ^0-ω interference term (third term on the right). The mass and width for ρ^0 were fixed to the PDG values. Background was estimated using a 6^{th} order polynomial (Pol6). The ρ^0 contribution is represented by a Breit-Wigner distribution (BW). To obtain the ρ^0 yield, the Breit-Wigner component obtained from the fit was integrated between the limits $2m_\pi$ to $M_\rho + 5\Gamma_\rho$.

The coherent cross section at mid-rapidity ($|y| < 0.5$) is $d\sigma/dy = 448 \pm 2$ (stat)$^{+38}_{-75}$ (sys) mb. Comparing to available model predictions, the Run 2 measurement is consistent with STARLIGHT [7], as was the Run 1 measurement. The GKZ model [8,9] overpredicts the data. The GM model [10], which agreed with the Run 1 measurement within uncertainties, overpredicts the ρ^0 cross section measured with Run 2 data.

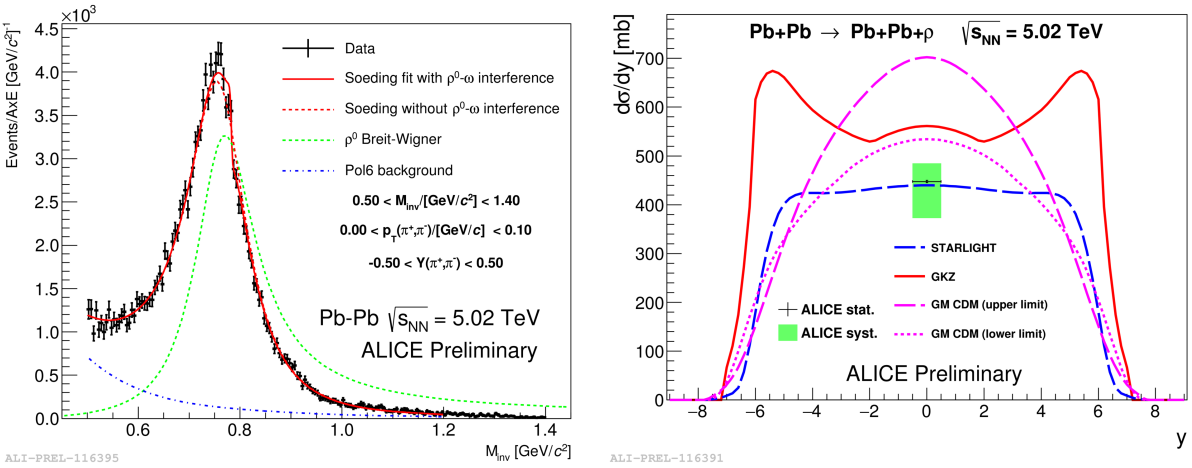

Fig. 1: (left) Run 2 $\pi^+\pi^-$ invariant mass spectrum and fits for the coherent ρ^0 analysis and (right) coherent ρ^0 cross section and available model predictions.

3.2 Coherent J/ψ

Current results for J/ψ in Run 2, at forward rapidity ($-4.0 < |y| < -2.5$) are shown in Fig. 2 for the di-muon channel. The p_T distribution is shown on the left along with Monte Carlo templates used to reproduce the distribution. The templates reproduce the data quite well. On the right, the di-muon

invariant mass spectrum is shown. The J/ψ and ψ(2S) peaks are fit with Crystal Ball functions. The ψ(2S) peak has a 3σ significance.

While Fig. 2 shows results for all the data at forward rapidity, the much higher statistics in Run 2 allow for more differential measurements. Results obtained for three regions of forward rapidity are shown in Fig. 3 (left). STARLIGHT [7] and models using the impulse approximation overpredict the data. As in Run 1, the cross sections measured in Run 2 are consistent with models that incorporate moderate nuclear gluon shadowing. The CGC model, LM IPsat [11], appears consistent with the data although the range reported for that model only reaches to one of the data points. The data are also consistent with the EPS09 leading order prediction [8] within uncertainties, as was the Run 1 data.

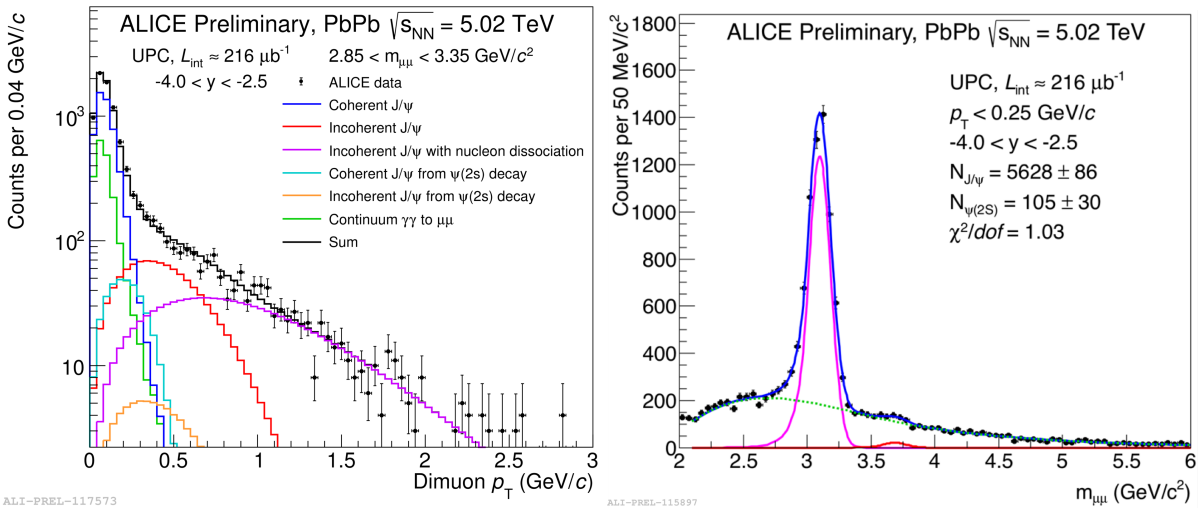

Fig. 2: (left) Run 2 coherent J/ψ p_T distribution and Monte Carlo templates that reproduce it well. (right) Di-muon invariant mass spectrum for J/ψ and ψ(2S) and fits using Run 2 data.

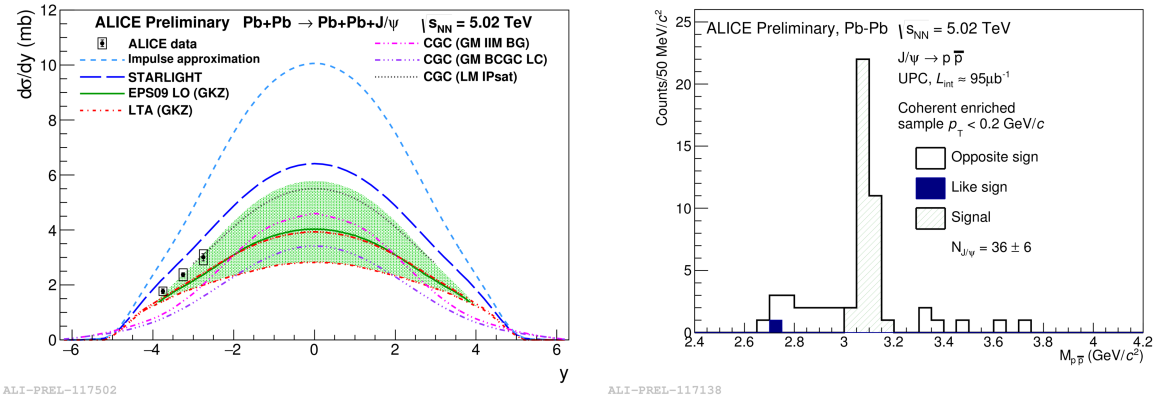

Fig. 3: (left) Cross section measurement, from Run 2, for coherent J/ψ production at forward rapidities with comparison to models. (right) Using Run 2 data, the first observed signal for J/$\psi \to p\bar{p}$ in UPC events.

Similar measurements for J/ψ at mid-rapidity are in progress. The mid-rapidity study will benefit from larger statistics compared to Run 1 and should provide access to $x \approx 5 \cdot 10^{-4}$. One particularly interesting measurement at mid-rapidity is shown in Fig. 3 (right). This is the first observation of J/$\psi \to p\bar{p}$ in ultra-peripheral collisions. There are 36$\pm$6 candidates although this signal may also contain entries from $\gamma\gamma \to p\bar{p}$.

3.3 Coherent ψ(2S)

The ψ(2S) signal, extracted from 95 μb^{-1} of data obtained in Run 2, are shown in Fig. 4 for ψ(2S)$\rightarrow$ $\mu^+\mu^-\pi^+\pi^-$ (left) and ψ(2S)$\rightarrow$ $e^+e^-\pi^+\pi^-$ (right). These results are for measurements at mid-rapidity.

During Run 1, the ratio of the mid-rapidity cross sections for J/ψ to ψ(2S) was found to be quite large, $0.34^{+0.08}_{-0.07}$ (stat+syst), compared to expectations from γp measurements and nearly all model predictions [4]. With the current results for Run 2, using J/ψ and ψ(2S) cross sections at forward rapidity, the ratio is found to be similar to that measured by HERA in γp interactions. The HERA result was 0.166$\pm$0.011 [12].

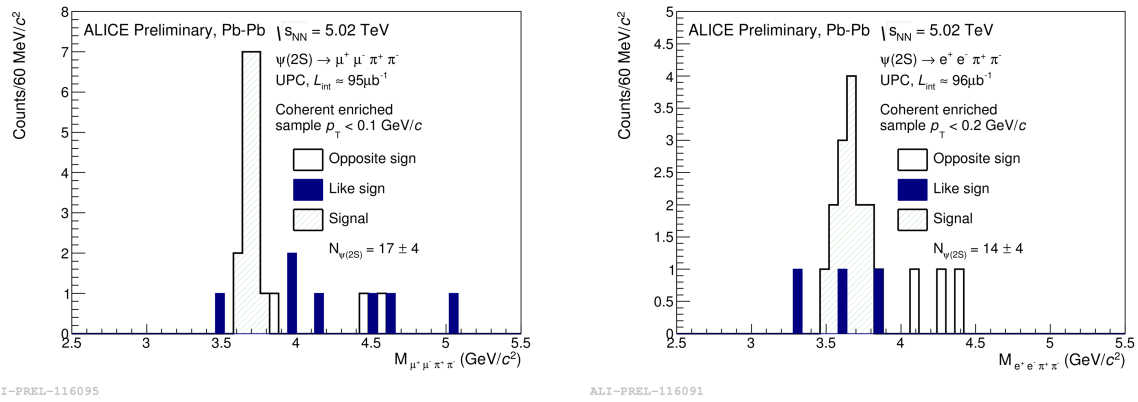

Fig. 4: Observed signals, in Run 2, for the ψ(2S) invariant mass spectra in the $\mu^+\mu^-\pi^+\pi^-$ channel (left) and $e^+e^-\pi^+\pi^-$ channel (right) at mid-rapidity.

4 Outlook and Summary

The latest UPC measurements from ALICE using data from Run 2 have significantly higher statistics compared to Run 1 allowing more differential measurements and smaller uncertainties, as well as opportunities for new measurements. The J/ψ cross section was measured in three forward rapidity ranges and the first observation of $J/\psi \rightarrow p\bar{p}$ in UPC events has been obtained. The ρ^0 cross section measurement places new constraints on the available models at mid-rapidity. The ratio of cross sections for J/ψ and ψ(2S) at forward rapidity is found to be consistent with results from HERA γp measurements and expectations from theory, much lower than the mid-rapidity measurement from Run 1.

Future plans for ALICE UPC measurements include studying events with different amounts of nuclear dissociation by counting very forward emitted neutrons in the ZDCs. In addition to ongoing measurements of ρ^0, J/ψ and ψ(2S), efforts are underway to measure additional particles.

Acknowledgements

This work has been supported in part by the U.S. Department of Energy, Office of Science.

References

[1] K. Aamodt *et al.*, JINST **3** (2008) S08002, http://dx.doi.org/10.1088/1748-0221/3/08/S08002.

[2] B. Abelev *et al.*, Int. J. Mod. Phys. A **29** (2014) 1430044, http://dx.doi.org/10.1142/S0217751X14300440.

[3] J. Adam *et al.*, JHEP **09** (2015) 095, http://dx.doi.org/10.1007/JHEP09(2015)095.

[4] J. Adam *et al.*, Phys. Lett. B **751** (2015) 358, http://dx.doi.org/10.1016/j.physletb.2015.10.040.

[5] B. Abelev *et al.*, Phys. Lett. B **718** (2013) 1273, http://dx.doi.org/10.1016/j.physletb.2012.11.059.

[6] E. Abbas *et al.*, Eur. Phys. J. C **73** (2013) 2617, http://dx.doi.org/10.1140/epjc/s10052-013-2617-1.

[7] S. R. Klein *et al.*, Comput. Phys. Commun. **212** (2017) 258, http://dx.doi.org/10.1016/j.cpc.2016.10.016.

[8] V. Guzey, E. Kryshen and M. Zhalov, Phys. Rev. C **93** (2016) 055206, http://dx.doi.org/10.1103/PhysRevC.93.055206.

[9] L. Frankfurt, V. Guzey, M. Strikman and M. Zhalov, Phys. Lett. B **752** (2016) 51, http://dx.doi.org/10.1016/j.physletb.2015.11.012.

[10] V. P. Goncalves and V. T. Machado, Phys. Rev. C **80** (2009) 054901, http://dx.doi.org/10.1103/PhysRevC.80.054901.

[11] T. Lappi and H. Mantysaari, Phys. Rev. C **87** (2013) 032201, http://dx.doi.org/10.1103/PhysRevC.87.032201.

[12] C. Adloff *et al.*, Phys. Lett. B **541** (2002) 251, http://dx.doi.org/10.1016/S0370-2693(02)02275-X.